Journal of Environmental Management 310 (2022) 114730

Contents lists available at ScienceDirect

Journal of Environmental Management

journal homepage: www.elsevier.com/locate/jenvman

Integral valorisation of walnut shells based on a three-step sequential delignification

Amaia Morales [a], Jalel Labidi [a,*], Patricia Gullón [b]

[a] Chemical and Environmental Engineering Department, University of the Basque Country UPV/EHU, Plaza Europa 1, 20018, San Sebastian, Spain
[b] Nutrition and Bromatology Group, Department of Analytical and Food Chemistry, Faculty of Food Science and Technology, University of Vigo, Ourense Campus, 32004, Ourense, Spain

ARTICLE INFO

Keywords:
Walnut shells
Biorefinery
Lignin
Sequential delignification
Valorisation

ABSTRACT

Walnut kernels represent no more than 50–60% of the total weight of the fruit, so the sum of walnut shells generated every year is immense. Nonetheless, these shells could be further valorised for the extraction of their main constituents following a biorefinery scheme. Hence, the objective of this work was an integral valorisation of walnut shells, which involved a sequential organosolv delignification (200 °C, 90 min, 70/30 v/v EtOH/H_2O, LSR 6:1) and several posterior non-isothermal hydrothermal treatments (180, 195 and 210 °C, LSR 8:1). Moreover, the spent solids after the aforementioned treatments were evaluated as possible sources of cellulose nanocrystals. The results showed that the sequential organosolv delignifications presented relative lignin yields up to 60%, which leaded to lignins that just differed on their molecular weight distributions. The hydrothermal treatments were efficient for the removal of still present hemicelluloses (14.7–71.8%), and permitted a successful cellulose nanocrystal obtaining whereas the spent solid from the delignification stages did not. Thus, this study presented an innovative strategy for the integral valorisation of walnut shells.

1. Introduction

The depletion of fossil resources together with the increasing demand for energy security have resulted in numerous social and ecological worries (Liao et al., 2020). Due to the aforementioned concerns, the current society needs an immediate changeover from a petroleum-based economy to a bio-based economy, which has motivated the interest on sustainable and green chemistry (Morales et al., 2019). In this framework, due to its renewable origin, biomass has arisen as a potential candidate and solution (Liao et al., 2020). It is a rich, low cost and abundant fount of biopolymers, sugars and chemicals, which are usually isolated and processed in biorefineries (Dragone et al., 2020; Liao et al., 2020). Hence, biomass and biorefineries are undergoing a significant boost worldwide.

Lignocellulosic materials together with carbohydrates, lignin and proteins are part of plant biomass (Iravani and Varma, 2020). Lignocellulosic materials constitute about the 70% of this type of biomass and they are composite materials mainly composed by three elements: cellulose, hemicelluloses and lignin (de Hoyos-Martínez et al., 2018; Iravani and Varma, 2020). These elements can be isolated and employed for the synthesis of new materials and chemicals. The high availability of lignocellulosic biomass is its main advantage, since around 1.3 billion tons of this biomass are generated in the world every year and only 3% are consumed for bioenergy, biochemicals and non-food related bio-products (Ubando et al., 2020). This amount of lignocellulosic biomass usually involves agro-alimentary and forestry residues, municipal wastes and several crops (de Hoyos-Martínez et al., 2018).

Among the agro-alimentary residues, nut shells are very abundant since tree nuts are highly consumed all over the world. The current demand for walnuts, together with hazelnuts, is very high because of their manifold alimentary applications (liquors, oils, nougats and chocolates, for instance) as along with their direct consumption. In Spain, for instance, the estimated per capita value of walnut kernel consumption is 0.3 kg/year (INC-International, 2018), following the Netherlands and France which consume 0.48 kg and 0.33 kg per capita each year, respectively. Nonetheless, with regard to the whole weight of the nut, walnut kernel represents less than the 60% (Hemmati et al., 2018; Orue et al., 2019), leading to the generation of tones of underestimated shells. Although they have recently begun to be used as natural dyes in textile industry (Ali and Nishkam, 2016; Doğan-Sağlamtimur et al., 2017; Mirjalili and Karimi, 2013), walnut shells (WNS) could be further valorised via a biorefinery approach since

* Corresponding author.
E-mail address: jalel.labidi@ehu.es (J. Labidi).

https://doi.org/10.1016/j.jenvman.2022.114730
Received 6 September 2021; Received in revised form 24 January 2022; Accepted 13 February 2022
Available online 21 February 2022

they are included in the lignocellulosic biomass.

Due to their composition (i.e. ≈ 30% hemicelluloses ≈ 20% cellulose, > 35% lignin, and < 15% others), from the biorefinery viewpoint, walnut shells could be a promising fount of lignin (Ahorsu et al., 2019; de Caprariis et al., 2017; Tan et al., 2019; Wartelle and Marshall, 2000). Lignin is a heterogeneous and intricate biopolymer constituted by disjointedly cross-linked phenylpropanoid monomers (coniferyl, sinapyl and coumaryl alcohols) (Iravani and Varma, 2020). In spite of its complex structure and its low water solubility, lignin has many interesting features that make it an appropriate backbone for the development of eco-friendly materials: it is biodegradable, biocompatible, it has antioxidant capacity and non-citotoxicity, (Iravani and Varma, 2020). This biopolymer is originally linked to other structural biopolymers such as hemicelluloses and cellulose, and it is, therefore, necessary to isolate it for further applications. Several treatments have been explored for the removal of lignin from biomass: acid-isolation, ionic liquids, sulphite and Kraft processes, alkaline treatment, organosolv delignification, etc. (Dávila et al., 2017). Organosolv treatments are an alternative to conventional Kraft and sulphite pulping methods since they are simple, sulphur-free processes, they require mild reaction conditions and present solvent-recyclability (Erdocia et al., 2014). Organic solvents are used in these treatments as the reaction medium, enabling the transformation of the input feedstock by the removing hemicelluloses and lignin due to the destruction of their linkages with cellulose (Jiang et al., 2018). Moreover, by hydrolysing this fraction in acidic medium, cellulose nanocrystals can be obtained, which present interesting properties such as biocompatibility and biodegradability and could be used as viscosity modulators at extrusion based 3D printing (Ji et al., 2020) or as reinforcing agents in composite materials (i.e. hydrogels, films…) (George and Sabapathi, 2015).

Taking the abovementioned into account, the principal objective of this work was to further explore the potentiality of walnut shells for an integral valorisation. To do so, a sequential triple organosolv delignification was proposed in order to maximise the lignin extraction and investigate the resulting yields and features of the extracted lignins after each stage. As far as we are concerned, there are scarce works on the delignification of walnut shells (Cebin et al., 2021; Hemmati et al., 2018; Tan et al., 2019; Zijlstra et al., 2019), and even less about a multiple-stage delignification of any lignocellulosic biomass (de Hoyos-Martínez et al., 2018). Moreover, as hemicelluloses were still present at the resultant solid, the latest was subjected to various hydrothermal treatments. Finally, the solids coming from the delignification and hydrothermal treatments were evaluated as possible sources of cellulose nanocrystals. To the best of our knowledge, the sequential organosolv delignification and a posterior hydrothermal treatment of walnut shells have not been studied yet, and there is little information about their use as a cellulose nanocrystal source (Hemmati et al., 2018). WNS were previously valorised through a typical combination of a pre-treatment, which was carried out with and without intensification, and an organosolv delignification step (Morales et al., 2021). In this case, a three-step organosolv delignification was performed to the raw biomass, and the resultant solid was treated for CNC obtaining, with and without a previous hydrothermal treatment. Thus, walnut shells were integrally valorised for the co-production of cellulose nanocrystals, lignin and hemicelluloses using green and sustainable biorefinery processes and contributing to circular economy.

2. Materials and methods

2.1. Materials

WNS used in this work were kindly provided by a farmer (Zaldibia, Guipúzcoa, Spain) and they were conditioned as in our previous work (Morales et al., 2021). Briefly, they were milled and sieved to a grain size between 1 and 2 mm and kept at ambient temperature in a dry place until use. The composition of WNS (18.75% glucan, 27.65% hemicelluloses, 33.25% Klason lignin, 3.14% acid soluble lignin, 2.45% ashes and 2.5% extractives) was determined in our previous study (Morales et al., 2021).

Acetic acid glacial (CH_3COOH, 99.5%), sulphuric acid (H_2SO_4, 96%) and sodium chlorite ($NaClO_2$, 25%) were supplied by PanReac Química SLU. Ethanol (C_2H_5OH, for synthesis, 99.9%) was provided by Scharlab S.L. All reagents were employed as supplied.

2.2. Sequential organosolv delignification of WNS

A sequential lignin extraction process was carried out to maximise the delignification of the WNS. For this aim, WNS were subjected to a first organosolv delignification from which a solid phase and black liquor were obtained. An aliquot of the solid phase was used for chemical characterization whereas the rest was subjected to a subsequent delignification stage. This cycle was repeated two other times, obtaining in this way three black liquors and a three times delignified solid as shown in Fig. 1.

The reaction parameters were chosen according to our previous study (Morales et al., 2021). The three sequential organosolv delignifications were carried out at 200 °C with an ethanol/water (70:30 v/v) mixture during 90 min and using a liquid to solid ratio (LSR) of 1:6. These treatments were carried out in a 1.5 L stainless steel reactor (5100 Parr coupled with a 4848 Parr PID controller). After the treatments, the liquid and solid phases were separated by vacuum filtration. The solids were initially washed with an ethanol/water 70:30 (v/v) mixture and then with distilled water until neutral pH. Afterwards, they were left to dry and weighted so as to calculate the solid yield. Lignin was precipitated from the black liquors by adding the double volume of acidified water (H_2SO_4 96% w/w to pH 2) with regard to the measured black liquor volume (de Hoyos-Martínez et al., 2018). The extracted lignins were washed till neutral pH with distilled water and they were air-dried afterwards.

Every recovered solid fraction and the precipitated lignins were chemically characterized as described in the next sections.

2.2.1. Characterisation of the solid fractions

The solid yield and the solubilisation of the raw material were determined by subjecting aliquots of all the air-dried solids to moisture and gravimetric analyses. Their composition was determined according to the TP-510-42618 standard of the National Renewable Energy Laboratory (NREL), as done in our previous study (Morales et al., 2021). Briefly, a two-step quantitative acid hydrolysis (QAH) was carried out, firstly adding 72% (w/w) H_2SO_4 at 30 °C for 1 h, and then with 4% (w/w) H_2SO_4 for the same time at 121 °C. After the QAH, the solid phase was weighed so as to determine the amount of Klason lignin, whereas the liquid phase was analyzed via High Performance Liquid Chromatography (HPLC) in order to quantify the present sugars (glucose, xylose and arabinose), galacturonic and acetic acid (Dávila et al., 2017). All the analyses were done by triplicate.

2.2.2. Lignin characterisation

The purity of the extracted lignins was measured as reported in our previous work (Morales et al., 2021). In brief, QAH was firstly done with 72% (w/w) H_2SO_4 at 30 °C during 1 h, and then at 121 °C with 12% (w/w) H_2SO_4 for another hour. The impurities in the liquor were analyzed by HPLC and the insoluble part was treated as Klason lignin (Erdocia et al., 2014). Further characterization was done according to previous works (Morales et al., 2020, 2021). These analyses included Pyrolysis-Gas Chromatography/Mass Spectrometry analysis (Py-GC/MS), High Performance Size Exclusion Chromatography (HPSEC), Fourier Transform Infrared Spectroscopy (FTIR), Thermogravimetric Analyses (TGA) and Differential Scanning Calorimetry (DSC).

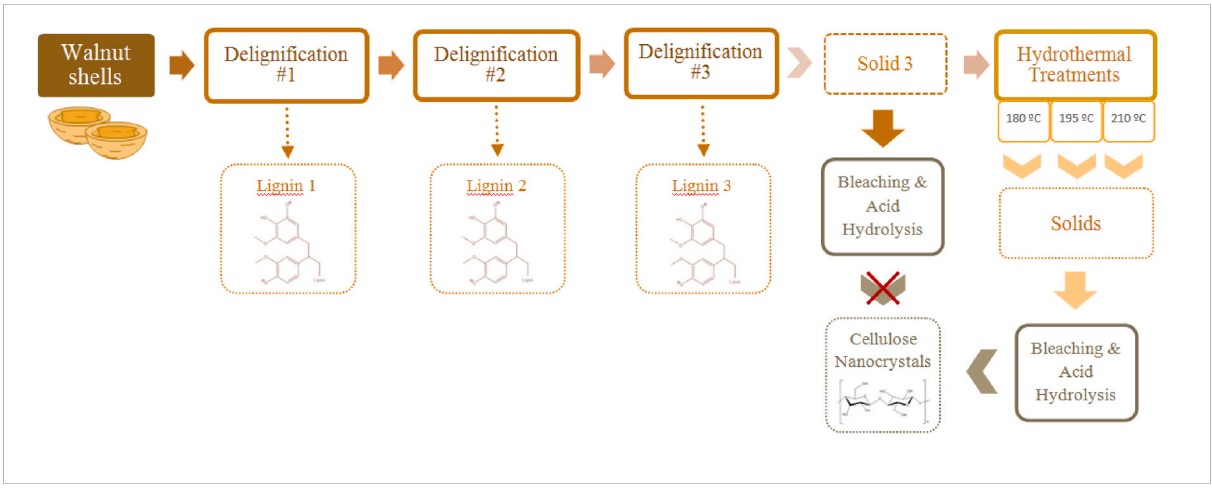

Fig. 1. Diagram of the developed biorefinery scheme for the integral valorisation of WNS.

2.3. Hydrothermal treatment of the three-times delignified WNS

The solid recovered after the triple organosolv delignification, was subjected to hydrothermal treatment in order to explore its efficiency on hemicelluloses solubilisation from a delignified solid. Non-isothermal autohydrolysis treatments were carried out by heating the solid-water mixtures up to three different temperatures (180, 195 and 210 °C) and cooling them down as soon as these temperatures were reached. The experiments were carried out with water in the abovementioned reactor, keeping a LSR of 8 kg solvent/kg dry solid. The obtained solids were characterised as described in Section 2.2.1., whereas the autohydrolysis liquors were subjected to a post-hydrolysis, as reported in our previous work (Morales et al., 2020, 2021). To compare the working conditions of the different experiments, the severity (S_0) of the hydrothermal treatments was calculated. This parameter has previously been defined by many authors (Dávila et al., 2016; Gullón et al., 2018; Morales et al., 2021).

2.4. Cellulose nanocrystal (CNC) production from the autohydrolysed and delignified WNS

CNC were produced following previously described methods (Morales et al., 2020, 2021). Briefly, the solid was firstly bleached for 2 h with acetic acid and sodium chlorite in an oil bath at 75 °C with magnetic stirring. Afterwards, the bleached solid and the liquid phase were vacuum filtered and the solid was rinsed with distilled water until neutral pH. The pulp was dried at 50 °C and an acid hydrolysis was carried out in an ultrasound bath (H_2SO_4 50% wt., 70 min, LSR of 15:1 and 55 °C) in an ultrasound bath. Subsequently, the slurry was filtered and rinsed with distilled water until pH 7. At last, an aqueous CNC suspension was prepared and introduced in an ultrasound bath in order to keep it stable. The production of CNC was verified via Atomic Force Microscopy (AFM) (Morales et al., 2020; Mujtaba et al., 2017).

3. Results and discussion

3.1. Sequential organosolv delignification of WNS

As abovementioned, the organic solvents employed during organosolv delignification remove hemicelluloses and lignin from biomass due to the breakage of the intermolecular bondages that link them to cellulose (Jiang et al., 2018). To our knowledge, other delignifications (i.e. alkaline and acidic) have been previously reported for WNS (Hemmati et al., 2018; Tan et al., 2019), but data about organosolv treatments is scarce (Morales et al., 2021; Zijlstra et al., 2019), and there is no information about multi-stage organosolv delignifications of this feedstock. Although multiple steps tend to make the processes costly and high energy demanding, it is sometimes necessary to take all these stages into account if the resulting output has great commercial interest. Thus, the aim of this triple-step delignification was to compare the yields and the properties of the isolated lignins.

The composition of the solids and the different extraction yields of the three cycles (overall, relative and total amount extracted yields) are shown in Tables 1 and 2, respectively. After the first organosolv delignification step, around a 55% of the initial solid was recovered. The composition of this solid was mainly 33% glucan, almost 20% xylan and 24.7% acid insoluble lignin. Comparing this composition with the one for raw WNS, it should be noted that the lignin content decreased around 8.6%, which, taking the solubilisation into account, meant a 59.56% of relative lignin removal (see Table 2). This yield was higher than that reported for eucalyptus (51.85%) under similar conditions (192.5 °C, 86 min and 65% ethanol aqueous mixture) (Romaní et al., 2019) but lower than the one found out for almond shells (79.95%) (de Hoyos-Martínez et al., 2018). The overall yield, however, was higher (19.90%) than that reported by the later authors (16.75%).

During the second organosolv delignification step, less than an 11% of the once-delignified solid was solubilised. The twice-delignified solid presented a higher glucan content (≈37%) than the previous one, accounting a total recovery of this fraction. Both the xylan content (18.56%) and the Klason lignin content (22.73%) got slightly reduced; nevertheless, the lignin removal still accounted a 17.65% of the one introduced in the reactor. This yield was again lower than the one reported for almond shells during the second extraction (27.17%) (de Hoyos-Martínez et al., 2018).

As a result of the third delignification step, almost a 94% of the introduced twice-delignified solid was recovered. The threes-delignified solid had higher glucan content (39.30%) than the twice-delignified one, also leading to a complete recovery of this component. The xylan fraction kept decreasing (16.17%); nonetheless, the Klason lignin remained unaltered, with just a 2.38% removal, which was much lower than that found for almond shells on the third delignification (15.86%) (de Hoyos-Martínez et al., 2018).

Taking the three delignification stages into account, the total amount of removed lignin was 67.40% of the lignin on the initial solid. This value was inferior to the one reported for almond shells by de Hoyos-Martinez et al., which could be directly attributed to the chemical composition of the employed feedstock (de Hoyos-Martínez et al., 2018).

From the obtained results it was observed that the first delignification yielded in high lignin extraction, whilst the extraction yield was

Table 1
Solubilisation, severity and chemical composition of the spent solids after the three delignifications and the autohydrolysis of the threes delignified solid.

Treatment		D1	D2	D3	D3+C180	D3+C195	D3+C210
Time (min)		90	90	90	51.05	65.00	71.40
Temperature (°C)		200	200	200	180	195	210
Severity		–	–	–	3.28	3.75	4.20
EtOH:H_2O (v/v)		70:30	70:30	70:30	–	–	–
Solubilisation (%)		45.27	10.55	5.91	5.08	16.64	18.66
Composition (%)	Glucan	32.98 ± 1.98	36.91 ± 3.22	39.3 ± 1.21	38.11 ± 3.6	46.65 ± 3.29	48.32 ± 0.39
	Xylan	19.81 ± 0.20	18.56 ± 0.12	16.17 ± 0.44	14.78 ± 0.55	8.87 ± 0.54	5.41 ± 0.58
	Arabinan	0	0	0	0	0	0
	Galacturonic acid	1.35 ± 0.20	1.37 ± 0.10	0.94 ± 0.10	0.67 ± 0.08	0.71 ± 0.02	0.69 ± 0.11
	Acetyl groups	2.39 ± 0.11	2.16 ± 0.11	1.65 ± 0.07	1.40 ± 0.09	0.90 ± 0.12	0.40 ± 0.10
	Klason lignin	24.69 ± 0.71	22.73 ± 0.92	23.59 ± 0.16	22.92 ± 0.18	22.70 ± 2.06	23.02 ± 2.71
	Others (by difference)	18.78	18.27	18.35	22.12	20.17	22.16

D1: delignified solid after the first delignification stage; **D2**: delignified solid after the second delignification stage; **D3**: delignified solid after the third delignification stage; **D3+C180**: threes delignified solid after conventional autohydrolysis at 180 °C; **D3+C195**: threes delignified solid after conventional autohydrolysis at 195 °C; **D3+C210**: threes delignified solid after conventional autohydrolysis at 210 °C.

Table 2
Different extraction yields of lignin.

Treatment	Overall Yield[a] (%)	Relative Yield[b] (%)	Total amount of lignin[c] (%)
D1	19.90	59.56	59.56
D2	4.36	17.65	66.70
D3	0.54	2.38	67.40

D1: first delignification stage; **D2**: second delignification stage; **D3**: third delignification stage.
[a] Amount of lignin extracted related to mass of used biomass.
[b] Amount of lignin extracted related to the lignin content in the biomass used.
[c] Percentage of lignin extracted after each related to the initial amount of lignin in biomass.

significantly lower in the subsequent delignifications. A similar trend was described by de Hoyos-Martínez et al. for almond shells (de Hoyos-Martínez et al., 2018). These authors stated that the reason for this behaviour was that as the percentage of lignin in the solid after each delignification stage was lesser, then the possibility of extracting lignin was also lower (de Hoyos-Martínez et al., 2018). However, this trend might also be related to the glycoside, benzyl ester and benzyl ether bondages between lignin and carbohydrates (You et al., 2015). In fact, it is believed that over 50% of lignin is covalently connected to them (You et al., 2015), which could lead to an easier extraction of non-covalently bonded lignin during the first treatment and, thus, higher yields. Then, as the non-covalent bondages become scarce in the treated solid, lignin gets more condensed due to stronger linkages and its extraction turns more complicated (de Hoyos-Martínez et al., 2018). Looking at the obtained results, it could be concluded that in terms of yields the second and specially the third delignification stages would not be worthwhile. However, the properties of the extracted lignins might justify the employment of the sequential processes.

3.2. Characterization of the lignins

3.2.1. Purity

The chemical composition of the sequentially extracted first two lignins (L1 and L2) is shown on the Supplementary data. It can be appreciated that, in terms of Klason lignin, the purity of the sample L1 was slightly higher than for L2 (94.40% and 93.47%, respectively). Although the values were insignificantly lower for the second extraction, no difference was seen on the sugar content and the purity was high in both cases. Therefore, it could be said that the sequential delignification did not alter the purity of the samples greatly. A similar result was reported by de Hoyos-Martínez et al. (de Hoyos-Martínez et al., 2018) for the sequential delignification of almond shells and it is also aligned with the purity obtained for organosolv WNS lignin previously (Morales et al., 2021).

3.2.2. Pyrolysis-Gas Chromatography/Mass Spectrometry analysis (Py-GC/MS)

The lignins obtained after sequential delignification were pyrolysed in order to examine their content in aromatic compounds and to estimate the syringol/guaiacol (S/G) ratio. This ratio is related to the structure of lignin and it depends on its source (Morales et al., 2018). The compounds with a greater abundance than 0.4% that have been identified and quantified are shown in the Supplementary Data.

The compounds that were identified after the pyrolysis of the three samples were mainly related to the lignin molecule, although they also presented some degradation products coming from fatty acids and carbohydrates. As in our previous work, the products coming from lignin were arranged into four categories depending on their structure: the ones coming from *p*-hydroxyphenyl (H), the ones coming from guaiacol (G), the ones derived from catechol (C) and the ones derived from syringol (S) (Chen et al., 2015; Morales et al., 2018, 2021). The sum of the identified compounds was close to 90% of the detected ones, and the S/G ratio was estimated in two ways: one excluding and the other one considering the C-type compounds as S-derived degradation products.

In general, the three lignins presented similar compounds in similar abundances. The aromatic compounds that were present in highest percentages were *p*-cresol (2.2–3.7%), guaiacol (6.7–7.1%), 4-methylguaiacol (10.7–12.6%), 3-methoxycatechol (5.3–6.6%), 4-ethylguaiacol (3.1–4.3%), 4-vinylguaiacol (4.7–6.3%), syringol (8.9–10.6%), 4-methylsyringol (8.4–12.6%) and acetoveratrone (2.6–3.7%). Most of these were in accordance with the ones obtained through the pyrolysis of the lignin coming from autohydrolysed WNS in our previous work (Morales et al., 2021). Apart from the abovementioned compounds, L2 and L3 lignins presented some different compounds such as syringaldehyde (3.2–3.6%), acetosyringone (2.5–3.2%) and homosyringic acid (0.9–1.0%), which L1 did not present. As expected, fatty acids were detected in large amounts (10.3–12.6%) in all the samples, as lipophilic extracts are usually present in nuts (Queirós et al., 2020).

Alike in our former study (Morales et al., 2021), between the classified groups, the G-type compounds were the most plentiful in all the samples. The S-type compounds were found in lower quantities followed by the H-type and finally the C-type ones. Therefore, the estimated S/G ratios were below 1 and ranged between 0.43 and 0.77, and between 0.60 and 0.95 considering the C-type compounds as S-type derivatives. These values are aligned with the S/G ratio reported in our previous work (Morales et al., 2021). It is known that β-O-4 bondages have the lowest dissociation energy their direct cleavage leads to the production of G-type phenolic compounds (Ma et al., 2016). Moreover, the S/G ratios were higher in L2 and L3 samples, which may be due to the fact that L1 was more heterogeneous and had more accessible linkages. Then, the lignin structure was more condensed and similar, which could

have leaded to a higher production of S-type compounds, making the S/G ratio be higher. The C-type derivatives resulted to be most abundant in L3, which may be ascribed to a higher degradation of lignin or, more specifically, of the S-type units (Ma et al., 2016). Although S/G ratios above 1 have been previously reported for whole walnut shells (Queirós et al., 2020), this ratio can vary depending on the isolation and pyrolysis methods employed (Tagami et al., 2019).

3.2.3. High Performance Size Exclusion Chromatography (HPSEC)

In order to define the molecular weight distribution of the extracted lignin samples as well as their polydispersity indexes HPSEC technique was employed. The results for the main molecular weight average (M_w), number average molecular weights (M_n) and polydispersity index (M_w/M_n) are displayed in Table S2 (Supplementary data) and Fig. 2a shows the obtained three chromatograms for L1, L2 and L3.

As it can be seen, the number average molecular weights ranged from 1600–2200 g/mol and the weight average molecular weights ranged between 8950–12,070 g/mol, approximately. These values were in between the ones published by other researchers for organosolv lignins (de Hoyos-Martínez et al., 2018; Domínguez et al., 2018; Erdocia et al., 2014) and are in accordance with the ones obtained previously (Morales et al., 2021).

Although there is no clear trend on the average molecular weights with the addition of delignification stages, the greatest percentage of each sample had each time a lower molecular weight i.e. the 64% of L1 had an average M_w of 13411 g/mol, the 92% of L2 was of around 13033 g/mol and the 93% of L3 presented 11725 g/mol. In the first stage it was easier to extract lignin fractions with lower molecular weight (266–1298 g/mol) probably due to the more heterogeneous lignin structure and the type of accessible linkages. However, as delignification stages augmented, the structure probably got more compact and it was more complex to break it down (de Hoyos-Martínez et al., 2018). Thus, the obtained lignin yield was also lower, which would be in accordance with the abovementioned results for delignification (see Section 3.1). The polydispersity indexes were similar in the three cases, but the most homogeneous lignin according to this index was L3 with a M_w/M_n of 5.16.

3.2.4. Fourier Transform Infrared Spectroscopy (FTIR)

As shown in Fig. 2b, the three lignin samples showed the same spectra, meaning that in spite of the number of the applied delignification stages, no structural change was provoked. The spectra showed the characteristic bands of organosolv lignin, which are in aligned with the ones described in previous works (Morales et al., 2021; Sequeiros and Labidi, 2017). The bands at low wavenumbers (829 and 1030 cm^{-1}) corresponded to β-glycosidic linkages from cellulosic impurities and hemicellulosic impurities (Sequeiros and Labidi, 2017), subsequently, which were in accordance with the results reported in Section 3.2.1. The bands appearing around 920 and 1125 cm^{-1} were attributed to the in plane C–H deformation of guaiacyl and syringyl units, respectively. The small shoulder at 1270 cm^{-1} in the three spectra may also be related to hemicellulosic impurities (Orue et al., 2019). The bands at 1220 and 1335 cm^{-1} were ascribed to the C–O stretching of the guaiacyl and syringyl rings, respectively, and the one around 1425 cm^{-1} to the aromatic skeletal vibration. The peak at 1460 cm^{-1} was characteristic of the asymmetric deformation of C–H groups, and the ones at 1510 and 1600 cm^{-1} were assigned to the C=C of aromatic skeletal vibrations. The signal at 1710 cm^{-1} was associated to the C=O stretch vibration in onjugated ketones, whereas the ones at 2840 and 2950 cm^{-1} represented the C–H vibration of methylene and methyl units. Finally, the

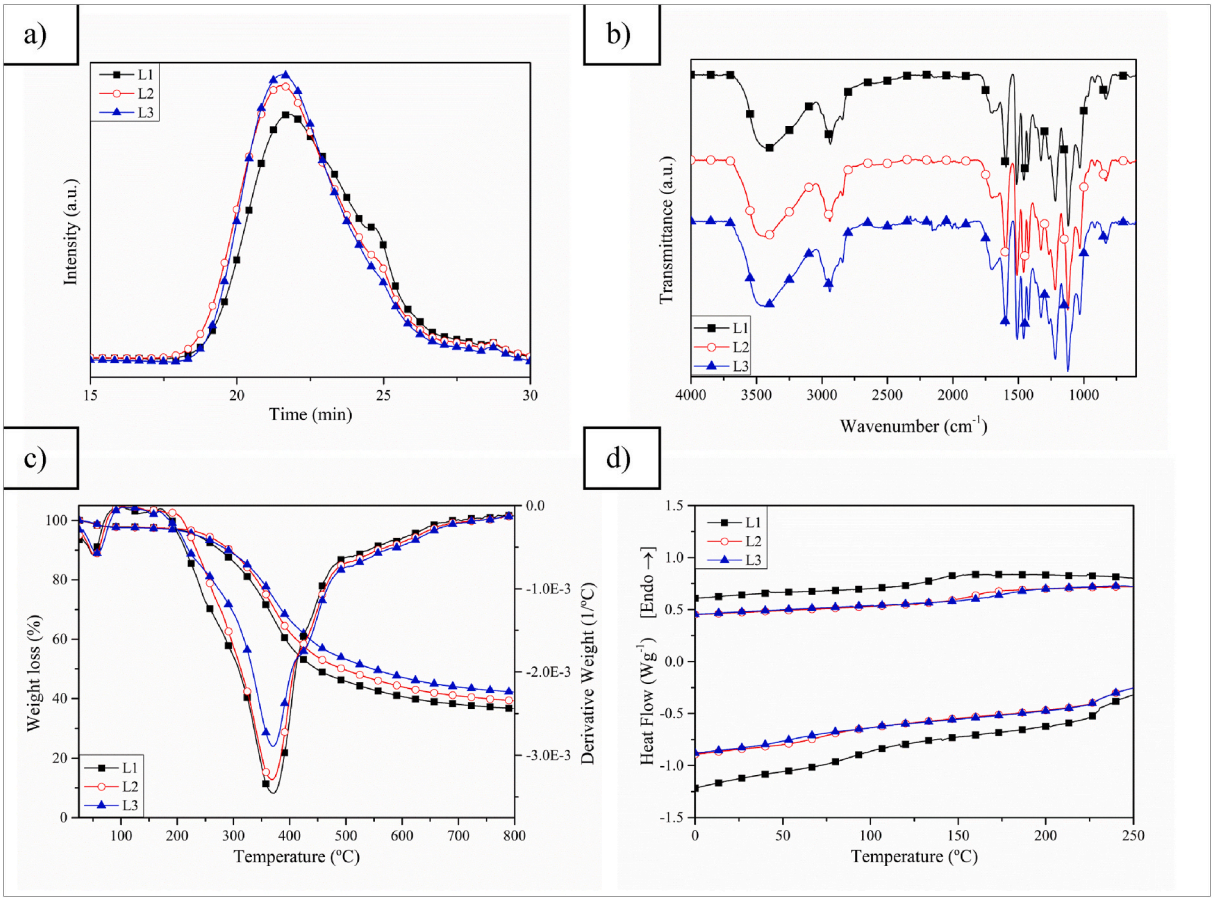

Fig. 2. a) Distributions of the molecular weights, b) FTIR spectra, c) TGA/DTG thermograms and d) DSC curves of the heating and cooling stages of L1, L2 and L3 lignins.

signal at 3460 cm^{-1} was related to the –OH stretching vibration.

3.2.5. Thermogravimetric Analyses (TGA)

The thermal behaviour of the sequentially extracted three lignins is shown in Fig. 2c by their TGA and DTGA curves. Four main degradation steps were seen for the three lignins. The first one around 50 °C corresponded to moisture evaporation (Morales et al., 2018), and it meant around a 2.5% of initial weight loss. Then, a shoulder around 245 °C was seen for the L1 sample, which decreased gradually for L2 and L3. This shoulder could be related to impurities or also to the decomposition of the lowest molecular weight fractions, which accounted 35% according to HPSEC analyses for L1 (Morales et al., 2018). The greatest degradation stage was observed around 375 °C for all the lignin samples. This value is also in agreement with the one reported by de Hoyos-Martínez et al.for organosolv lignins (de Hoyos-Martínez et al., 2018). Moreover, these authors attributed the wideness of the main degradation stage to the polidispersity of the lignins, which would also make sense in this case, since the peak was narrower as the lignins were less heterogeneous (de Hoyos-Martínez et al., 2018). The last degradation shoulder was appreciated around 430 °C, which could be related to the demethoxylation reactions in aromatic rings (Liu et al., 2016). At 800 °C a 37, 39 and 42% of char was left by L1, L2 and L3 samples, respectively. This increase on the char content could be ascribed to a higher inorganic content or lower purity as more delignification stages were performed. A similar result was also observed by other authors (de Hoyos-Martínez et al., 2018). In conclusion, the extracted lignins were more thermally stable as their homogeneity increased, but at the same time their purity was lower and the char left also was greater.

3.2.6. Differential Scanning Calorimetry (DSC)

DSC analyses were done in order to study the thermal properties of the sequentially extracted lignins. According to García et al., the glass transition temperature (T_g) of lignin tends to vary from 80 to 180 °C (García et al., 2012). This change can be related to many factors such as its source and the extraction method, which can at the same time affect the impurity content as well as the crosslinking degree and the molecular weight (García et al., 2012). The thermograms for samples L1, L2 and L3 are displayed in Fig. 2d. As seen, the three lignins presented a similar behaviour when heating them from −25 °C to 250 °C. The T_g of L1 sample seemed to appear around 150 °C, whereas the ones for L2 and L3 were seen around 160 °C. This shift on the T_g could be attributed to the homogeneity of the samples; hence, as the lignin fractions were more similar, were more entangled and lacked of low molecular weight fractions, the flowing facility decreased. No other significant variations were appreciated from the three thermograms.

3.3. Hydrothermal treatment of the three-times delignified WNS

After the three delignification stages, the solid was subjected to several non-isothermal hydrothermal treatments. To our knowledge, it is the first time that an autohydrolysis stage is performed after an organosolv delignification treatment. Three different temperatures were employed for the autohydrolysis of this solid: 180, 195 and 210 °C. The compositions of the spent solids are shown in Table 1 (D3+C180, D3+C195 and D3+C210, respectively). It was seen that the solubilisation of the solid presented a meaningful increase when rising the temperature from 180 to 195 °C, which leaded to severity factors of 3.28 and 3.75, respectively. Nevertheless, when the process was carried out at 210 °C, the severity factor increased to 4.20 but the solubilised solid was only 2% higher than that at 195 °C. The glucan and xylan contents on the composition of the solids at 180 and 195 °C were significantly different. In fact, taking the solubilisation into account, the elimination of the hemicellulosic fraction incremented from 14.74% at 180 °C, to 53.43% at 195 °C and then to 71.82% at 210 °C.

The previous was confirmed by the composition of the extracted liquors, of which the composition is shown in Table S3 (Supplementary data) and the corresponding concentrations of extracted monosaccharides (glucose, xylose and arabinose), oligosaccharides (GOS, XOS and ArOS) and degradation compounds (acetic acid, furfural and HMF) are shown in Fig. S2 (Supplementary data). It was seen that the substrate conversion into NVC doubly augmented from 180 to 195 °C, whereas this change was lower from 195 to 210 °C. The VC, however, were slightly higher at 195 °C (1.16 vs. 1.06%), but the conversion of acetyl groups into acetic acid was more notable at 210 °C (4.70%), in which more degradation products were expected to appear. At the lowest temperature, low xylan to xylose conversion was detected (0.28%), but the conversion of xylan into xylooligosaccharides (XOS) and acetyl groups of oligosaccharides (AcOS) were abundant (20.71 and 11.59%, respectively). At 195 °C, the xylan conversion into XOS increased to 34.81% and, thus, the xylose conversion was also enhanced (6.56%). These conversions leaded to a concentration of 7.83 g/L and 1.47 g/L of XOS and xylose, respectively (see Fig. S2a). Dávila et al. reported higher concentrations of XOS (10 g/L), but lower concentrations of xylose (0.1 g/L) at 195 °C for vine shoots (Dávila et al., 2016). Moreover, the acetyl group conversion into AcOS augmented to 24.28% and acetic acid also began to appear. After the hydrothermal treatment at 210 °C, XOS were significantly reduced (1.07 g/L) due to their conversion into xylose (9.98 g/L). Gullón et al. also reported the maximum xylose yield from chestnut shells at 210 °C (Gullón et al., 2018). In addition, less AcOS conversion was accounted and the generation of acetic acid was promoted (1.53 g/L). Furthermore, no glucooligosaccharides or glucose was detected below 210 °C, which could be related to the beginning of the degradation of cellulose at this temperature. It is well known that hydrothermal treatments cause the breakage of bonds in biomass and the dissolved components firstly exist as oligomers principally. A higher degradation of hemicelluloses and cellulose derivatives can generate monosaccharides (such as glucose and xylose), small organic acids and furan derived chemicals (Jiang et al., 2018). Therefore, the lack of products such as HMF and furfural at 180 °C and the raise in their concentrations in the following treatments would confirm the previous statement. The degradation products resulted in a joint concentration of 0.47 and 3.60 g/L at 195 and 210 °C, subsequently (see Fig. S2b).

3.4. Cellulose nanocrystal (CNC) production from the delignified and autohydrolysed WNS

The spent solids from the third delignification stage and after hydrothermal treatment at 195 °C, which had yielded the highest XOS production and low concentrations of degradation products, underwent a bleaching step and an acid hydrolysis so as to obtain CNC. The AFM images presented in Fig. 3 confirmed a successful CNC production for the solid after hydrothermal process whereas for the solid after the third delignification stage did not. This could be related to the hemicellulosic presence, which may hinder the generation of nanocrystals. It is known that the acid hydrolysis humbles hemicelluloses and amorphous cellulose for the production of CNC, but the efficiency of this process may be limited due to the presence of non-CNC compounds (Beyene et al., 2020). In fact, Beyene et al. verified that a hydrothermal treatment before the acid hydrolysis improved the yield of CNC obtaining (Beyene et al., 2020).

The images for the obtained CNC together with their typical surface profile are shown in Fig. 3. The morphology and size of the produced CNC were deduced from these micrographs. The obtained CNC showed the typical morphology, i.e. sharp contours and rod-like structure. The estimated average length (L) and diameter (D) were 369.53 ± 123.71 and 36.81 ± 6.38, leading to an average aspect ratio (L/D) of 10.40 ± 3.90. The results for L and D were slightly lower than those reported for WNS previously (Morales et al., 2021). Nevertheless, the change in the aspect ratio was insignificant (10.40 vs. 10.77). In general, the obtained data were similar to the results reported for lignocellulosic-biomass CNC (Babu Perumal et al., 2018; Herrera et al., 2016; Mujtaba et al., 2017;

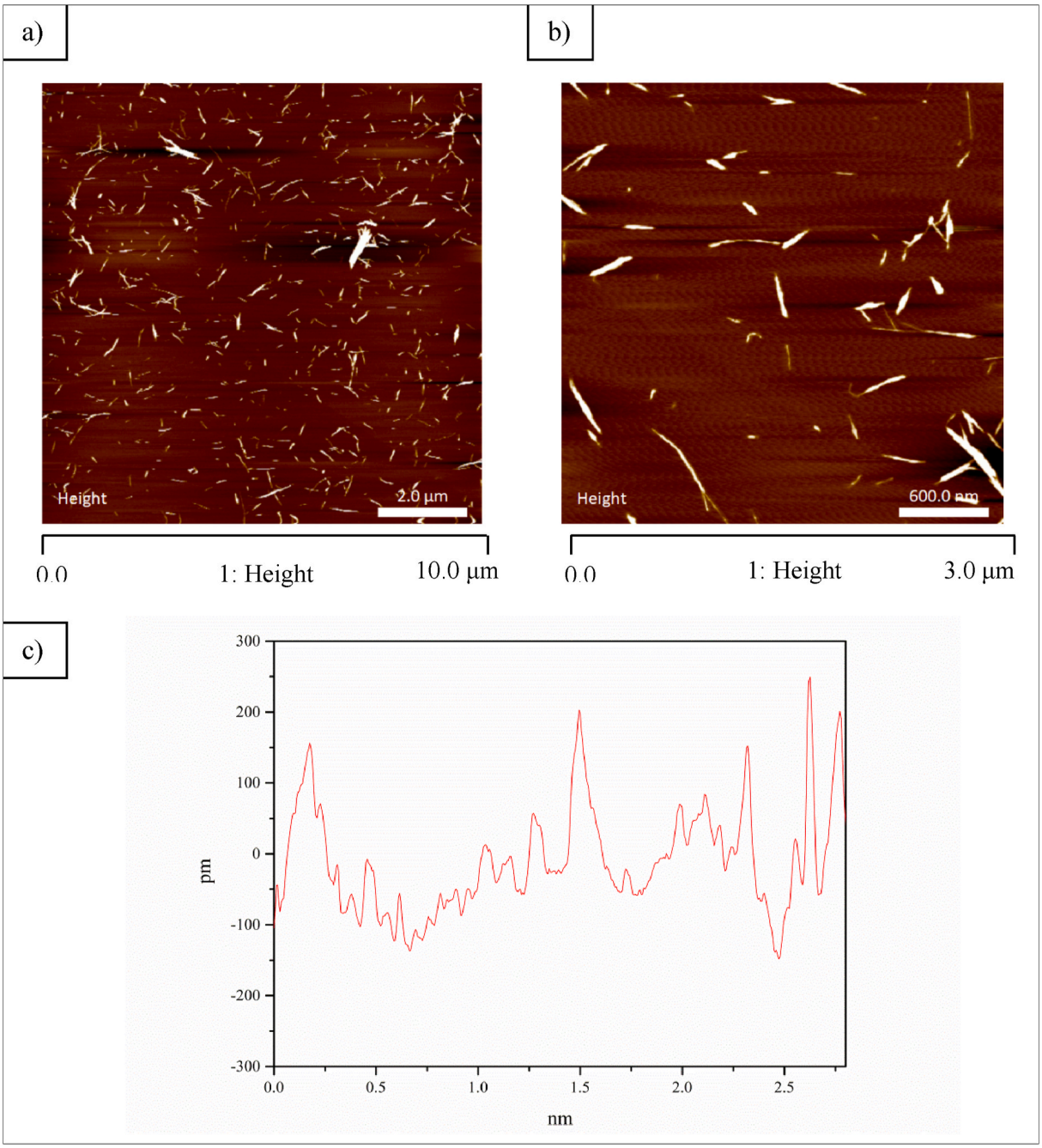

Fig. 3. AFM images (a and b) and surface profile (c) along the sample in the marked area of 2D AFM images of the CNC obtained from D3+C195 solid.

Xiao et al., 2019).

Fig. 3c shows that the roughness of the studied surface. The maximum deviation was of around 250 p.m., which is less than 1 nm, meaning that the produced CNC were much more homogeneous and smaller than the ones obtained previously (Morales et al., 2021).

3.5. Comparative analysis with previous works

As aforementioned, a previous work on the integral valorisation of walnut shells was carried out (Morales et al., 2021). The experimental scheme of the later consisted of a hydrothermal pre-treatment (carried out by both microwave assisted heating and conventional heating), followed by an organosolv delignification carried out in a conventional reactor. Comparing the present and the previous works, it can be said that the overall yield of the first organosolv step was higher after a pre-treatment stage (28.7% vs. 19.9%). In fact, the addition of the yields obtained after the three delignification steps in this works did not surpass the one obtained in the previous work. Nevertheless, the present valorisation procedure enabled the obtaining of more homogeneous lignins with higher molecular weights, which depending on the application could be desired. Regarding the hydrothermal process, the one at 200 °C before the organosolv treatment in the previous work permitted twofold the highest XOS extraction yield in the present work (at 195 °C), which could be related to the elimination of the hemicellulosic fraction during the three delignification stages. Actually, it should be highlighted that the hemicelluloses that were removed during the delignification stages (> 50% of the hemicelluloses in the initial solid) were not recovered, which is not convenient if the valorisation of this fraction is aimed. As for the CNC, the present process enabled the production of more homogeneous and smaller nanocrystals than the ones in the

previous work. Moreover, it was demonstrated that a hydrothermal process (before or after the delignification step) is necessary if the production of CNC is desired.

Looking at the previous comparison, it could be said that the valorisation route presented in this work could be simplified due to the low delignification yields obtained from the second organosolv treatment on and the similarity of the isolated lignins. In fact, the addition of these two organosolv stages would increase the energetic demand and time, which would result into an unnecessary increase on the cost of the process. However, this work gives an idea of the main differences between the proposed integral valorisation routes, and would be useful depending on the aimed final products and their applications.

4. Conclusions

In this work a complete valorisation of WNS was proposed through a sequential three-step organosolv delignification, subsequent hydrothermal treatments and CNC production. On the one hand, it was observed that the sequential delignification steps enabled the production of cellulose-rich pulps coupled with very pure lignin streams (93–94%). The first delignification stage resulted in the highest yields of lignin (≈ 60% removal). Moreover, the lignins from the next extractions were very similar to the first one in structure, composition and thermal stability terms. The main variation was observed in their molecular weights, which got lowered but more homogeneous from step to step and their M_w ranged from 8950–12,070 g/mol. From the subsequent hydrothermal treatments, the one at 210 °C presented the highest hemicelluloses removal (71.8%), while the highest XOS extraction was performed at 195 °C (≈ 35%). Moreover, the bleached pulp from the latter process leaded to a successful CNC production whereas the bleached solid from the third delignification process did not, which was ascribed to the presence of hemicelluloses. As far as we know, it was the first time that walnut shells were integrally valorised though a sequential delignification and a subsequent autohydrolysis, which leaded to a successful production of CNC and demonstrated that the presence of hemicelluloses affect their production. Although the employment of the additional two delignification stages might be questionable, the isolated fractions seem to be promising in many application fields such as the synthesis of new composite materials, chemicals, prebiotics or 3D printing.

Credit author statement

Amaia Morales: Methodology, Investigation, Data curation, Writing – original draft. Jalel Labidi: Resources, Writing- Reviewing and Editing, Funding acquisition. Patricia Gullón: Conceptualization, Validation, Supervision, Writing- Reviewing and Editing,

Declaration of competing interest

The authors declare that they have no known competing financial interests or personal relationships that could have appeared to influence the work reported in this paper.

Acknowledgements

The authors would like to thank the Department of Education of the Basque Government (IT1008-16) for the financial support. A. Morales would like to thank the University of the Basque Country (Training of Researcher Staff, PIF17/207). The authors would like to thank SGIker for the provided technical and human support (UPV/EHU/ERDF, EU).

Appendix A. Supplementary data

Supplementary data to this article can be found online at https://doi.org/10.1016/j.jenvman.2022.114730.

References

Ahorsu, R., Cintorrino, G., Medina, F., Constantí, M., 2019. Microwave processes: a viable technology for obtaining xylose from walnut shell to produce lactic acid by Bacillus coagulans. J. Clean. Prod. 231, 1171–1181. https://doi.org/10.1016/j.jclepro.2019.05.289.

Ali, A., Nishkam, A., 2016. Extraction of dye from walnut shell and dyeing of natural fibre. IOSR J. Polym. Text. Eng. 3, 7–9. https://doi.org/10.9790/019X-03010709.

Babu Perumal, A., Selvam Sellamuthu, P., Nambiar, R.B., Rotimi Sadiku, E., 2018. Applied Surface Science Development of polyvinyl alcohol/chitosan bio-nanocomposite films reinforced with cellulose nanocrystals isolated from rice straw. Appl. Surf. Sci. 449, 591–602. https://doi.org/10.1016/j.apsusc.2018.01.022.

Beyene, D., Chae, M., Vasanthan, T., Bressler, D.C., 2020. A biorefinery strategy that introduces hydrothermal treatment prior to acid hydrolysis for Co-generation of furfural and cellulose nanocrystals. Front. Chem. 8, 1–11. https://doi.org/10.3389/fchem.2020.00323.

Cebin, A.V., Ralet, M.C., Vigouroux, J., Karača, S., Martinić, A., Komes, D., Bonnin, E., 2021. Valorisation of walnut shell and pea pod as novel sources for the production of xylooligosaccharides. Carbohydr. Polym. 263, 117932. https://doi.org/10.1016/j.carbpol.2021.117932.

Chen, L., Wang, X., Yang, H., Lu, Q., Li, D., Yang, Q., Chen, H., 2015. Study on pyrolysis behaviors of non-woody lignins with TG-FTIR and Py-GC/MS. J. Anal. Appl. Pyrolysis 113, 499–507. https://doi.org/10.1016/j.jaap.2015.03.018.

Dávila, I., Gordobil, O., Labidi, J., Gullón, P., 2016. Assessment of suitability of vine shoots for hemicellulosic oligosaccharides production through aqueous processing. Bioresour. Technol. 211, 636–644. https://doi.org/10.1016/j.biortech.2016.03.153.

Dávila, I., Gullón, P., Andrés, M.A., Labidi, J., 2017. Coproduction of lignin and glucose from vine shoots by eco-friendly strategies: toward the development of an integrated biorefinery. Bioresour. Technol. 244, 328–337. https://doi.org/10.1016/j.biortech.2017.07.104.

de Caprariis, B., De Filippis, P., Petrullo, A., Scarsella, M., 2017. Hydrothermal liquefaction of biomass: influence of temperature and biomass composition on the bio-oil production. Fuel 208, 618–625. https://doi.org/10.1016/j.fuel.2017.07.054.

de Hoyos-Martínez, P.L., Erdocia, X., Charrier-El Bouhtoury, F., Prado, R., Labidi, J., 2018. Multistage treatment of almonds waste biomass: characterization and assessment of the potential applications of raw material and products. Waste Manag. 80, 40–50. https://doi.org/10.1016/j.wasman.2018.08.051.

Doğan-Sağlamtimur, N., Turaç, E., Arabacioğlu, R., Çivioğlu, T., 2017. Production of dye from green and brown walnut shells for leather coloration. Period. Eng. Nat. Sci. 5, 224–230. https://doi.org/10.21533/pen.v5i2.135.

Domínguez, J.C., Santos, T.M., Rigual, V., Oliet, M., Alonso, M.V., Rodriguez, F., 2018. Thermal stability, degradation kinetics, and molecular weight of organosolv lignins from Pinus radiata. Ind. Crop. Prod. 111, 889–898. https://doi.org/10.1016/j.indcrop.2017.10.059.

Dragone, G., Kerssemakers, A.A.J., Driessen, J.L.S.P., Yamakawa, C.K., Brumano, L.P., Mussatto, S.I., 2020. Innovation and strategic orientations for the development of advanced biorefineries. Bioresour. Technol. 302, 122847. https://doi.org/10.1016/j.biortech.2020.122847.

Erdocia, X., Prado, R., Corcuera, M.Á., Labidi, J., 2014. Effect of different organosolv treatments on the structure and properties of olive tree pruning lignin. J. Ind. Eng. Chem. 20, 1103–1108. https://doi.org/10.1016/j.jiec.2013.06.048.

García, A., González Alriols, M., Spigno, G., Labidi, J., 2012. Lignin as natural radical scavenger. Effect of the obtaining and purification processes on the antioxidant behaviour of lignin. Biochem. Eng. J. 67, 173–185. https://doi.org/10.1016/j.bej.2012.06.013.

George, J., Sabapathi, S.N., 2015. Cellulose nanocrystals: synthesis, ftional properties, and applications. Nanotechnol. Sci. Appl. 8, 45–54. https://doi.org/10.2147/NSA.S64386.

Gullón, B., Eibes, G., Dávila, I., Moreira, M.T., Labidi, J., Gullón, P., 2018. Hydrothermal treatment of chestnut shells (Castanea sativa) to produce oligosaccharides and antioxidant compounds. Carbohydr. Polym. 192, 75–83. https://doi.org/10.1016/j.carbpol.2018.03.051.

Hemmati, F., Jafari, S.M., Kashaninejad, M., Barani Motlagh, M., 2018. Synthesis and characterization of cellulose nanocrystals derived from walnut shell agricultural residues. Int. J. Biol. Macromol. 120, 1216–1224. https://doi.org/10.1016/j.ijbiomac.2018.09.012.

Herrera, N., Salaberria, A.M., Mathew, A.P., Oksman, K., 2016. Plasticized polylactic acid nanocomposite films with cellulose and chitin nanocrystals prepared using extrusion and compression molding with two cooling rates: effects on mechanical, thermal and optical properties. Compos. Part A Appl. Sci. Manuf. 83, 89–97. https://doi.org/10.1016/j.compositesa.2015.05.024.

INC-International, 2018. Nut & Dried Fruit. Statistical Yearbook 2018-2019.

Iravani, S., Varma, R.S., 2020. Greener synthesis of lignin nanoparticles and their applications. Green Chem. 22, 612–636. https://doi.org/10.1039/c9gc02835h.

Ji, A., Zhang, S., Bhagia, S., 2020. 3D Printing of Biomass-Derived Composites: Application and Characterization Approaches 21698–21723. https://doi.org/10.1039/D0RA03620J.

Jiang, Z., Zhao, P., Hu, C., 2018. Controlling the cleavage of the inter- and intra-molecular linkages in lignocellulosic biomass for further biorefining: a review. Bioresour. Technol. 256, 466–477. https://doi.org/10.1016/j.biortech.2018.02.061.

Liao, J.J., Hanis, N., Latif, A., Trache, D., Brosse, N., Hussin, M.H., 2020. Current advancement on the isolation , characterization and application of lignin. Int. J. Biol. Macromol. 162, 985–1024. https://doi.org/10.1016/j.ijbiomac.2020.06.168.

Liu, C., Hu, J., Zhang, H., Xiao, R., 2016. Thermal conversion of lignin to phenols: relevance between chemical structure and pyrolysis behaviors. Fuel 182, 864–870. https://doi.org/10.1016/j.fuel.2016.05.104.

Ma, Z., Sun, Q., Ye, J., Yao, Q., Zhao, C., 2016. Study on the thermal degradation behaviors and kinetics of alkali lignin for production of phenolic-rich bio-oil using TGA-FTIR and Py-GC/MS. J. Anal. Appl. Pyrolysis 117, 116–124. https://doi.org/10.1016/j.jaap.2015.12.007.

Mirjalili, M., Karimi, L., 2013. Extraction and characterization of natural dye from green walnut shells and its use in dyeing polyamide: focus on antibacterial properties. J. Chem. https://doi.org/10.1155/2013/375352.

Morales, A., Andrés, M.Á., Labidi, J., Gullón, P., 2019. UV–vis protective poly(vinyl alcohol)/bio-oil innovative films. Ind. Crop. Prod. 131 https://doi.org/10.1016/j.indcrop.2019.01.071.

Morales, A., Gullón, B., Dávila, I., Eibes, G., Labidi, J., Gullón, P., 2018. Optimization of alkaline pretreatment for the co-production of biopolymer lignin and bioethanol from chestnut shells following a biorefinery approach. Ind. Crop. Prod. 124 https://doi.org/10.1016/j.indcrop.2018.08.032.

Morales, A., Hernández-Ramos, F., Sillero, L., Fernández-Marín, R., Dávila, I., Gullón, P., Erdocia, X., Labidi, J., 2020. Multiproduct biorefinery based on almond shells: impact of the delignification stage on the manufacture of valuable products. Bioresour. Technol. 315 https://doi.org/10.1016/j.biortech.2020.123896.

Morales, A., Labidi, J., Gullón, P., 2021. Hydrothermal treatments of walnut shells: a potential pretreatment for subsequent product obtaining. Sci. Total Environ. 764, 142800. https://doi.org/10.1016/j.scitotenv.2020.142800.

Mujtaba, M., Salaberria, A.M., Andres, M.A., Kaya, M., Gunyakti, A., Labidi, J., 2017. Utilization of flax (Linum usitatissimum) cellulose nanocrystals as reinforcing material for chitosan films. Int. J. Biol. Macromol. 104, 944–952. https://doi.org/10.1016/j.ijbiomac.2017.06.127.

Orue, A., Eceiza, A., Arbelaiz, A., 2019. The use of alkali treated walnut shells as filler in plasticized poly(lactic acid) matrix composites. Ind. Crop. Prod. 111993. https://doi.org/10.1016/j.indcrop.2019.111993.

Queirós, C.S.G.P., Cardoso, S., Lourenço, A., Ferreira, J., Miranda, I., Lourenço, M.J.V., Pereira, H., 2020. Characterization of walnut, almond, and pine nut shells regarding chemical composition and extract composition. Biomass Convers. Biorefinery 10, 175–188. https://doi.org/10.1007/s13399-019-00424-2.

Romaní, A., Larramendi, A., Yáñez, R., Cancela, Á., Sánchez, Á., Teixeira, J.A., Domingues, L., 2019. Valorization of Eucalyptus nitens bark by organosolv pretreatment for the production of advanced biofuels. Ind. Crop. Prod. 132, 327–335. https://doi.org/10.1016/j.indcrop.2019.02.040.

Sequeiros, A., Labidi, J., 2017. Characterization and determination of the S/G ratio via Py-GC/MS of agricultural and industrial residues. Ind. Crop. Prod. 97, 469–476. https://doi.org/10.1016/j.indcrop.2016.12.056.

Tagami, A., Gioia, C., Lauberts, M., Budnyak, T., Moriana, R., Lindström, M.E., Sevastyanova, O., 2019. Solvent fractionation of softwood and hardwood kraft lignins for more efficient uses: compositional, structural, thermal, antioxidant and adsorption properties. Ind. Crop. Prod. 129, 123–134. https://doi.org/10.1016/j.indcrop.2018.11.067.

Tan, M., Ma, L., Rehman, M.S.U., Ahmed, M.A., Sajid, M., Xu, X., Sun, Y., Cui, P., Xu, J., 2019. Screening of acidic and alkaline pretreatments for walnut shell and corn stover biorefining using two way heterogeneity evaluation. Renew. Energy 132, 950–958. https://doi.org/10.1016/j.renene.2018.07.131.

Ubando, A.T., Felix, C.B., Chen, W.H., 2020. Biorefineries in circular bioeconomy: a comprehensive review. Bioresour. Technol. 299 https://doi.org/10.1016/j.biortech.2019.122585.

Wartelle, L.H., Marshall, W.E., 2000. Citric acid modified agricultural by-products as copper ion adsorbents. Adv. Environ. Res. 4, 1–7. https://doi.org/10.1016/S1093-0191(00)00002-2.

Xiao, Y., Liu, Y., Wang, X., Li, M., Lei, H., Xu, H., 2019. Cellulose nanocrystals prepared from wheat bran: characterization and cytotoxicity assessment. Int. J. Biol. Macromol. 140, 225–233. https://doi.org/10.1016/j.ijbiomac.2019.08.160.

You, T.T., Zhang, L.M., Zhou, S.K., Xu, F., 2015. Structural elucidation of lignin-carbohydrate complex (LCC) preparations and lignin from Arundo donax Linn. Ind. Crop. Prod. 71, 65–74. https://doi.org/10.1016/j.indcrop.2015.03.070.

Zijlstra, D.S., Analbers, C.A., de Korte, J., Wilbers, E., Deuss, P.J., 2019. Efficient mild organosolv lignin extraction in a flow-through setup yielding lignin with high β-O-4 content. Polymers 11, 14–17. https://doi.org/10.3390/polym11121913.